Sensors and Materials, Vol. 32, No. 4 (2020) 1405–1410
MYU Tokyo

S & M 2187

Evaluation of Optically Stimulated Luminescence Properties of Tm-doped $NaMgF_3$ Single Crystals

Yuma Takebuchi,* Hiroyuki Fukushima, Takumi Kato,
Daisuke Nakauchi, Noriaki Kawaguchi, and Takayuki Yanagida

Division of Materials Science, Nara Institute of Science and Technology (NAIST), Ikoma, Nara 630-0192, Japan

(Received November 20, 2019; accepted February 25, 2020)

Keywords: storage phosphor, OSL, $NaMgF_3$

Undoped and Tm-doped $NaMgF_3$ single crystals were synthesized and investigated in terms of their scintillation and optically stimulated luminescence (OSL) properties. The synthesized samples were confirmed by X-ray diffraction to be a single-phase $NaMgF_3$. The Tm-doped sample showed an X-ray-induced scintillation spectrum characterized by sharp emission lines owing to the 4f–4f transitions of Tm^{3+}. The OSL spectrum of the Tm-doped sample also showed emission at around 360 nm, which was ascribed to the 4f–4f transitions of Tm^{3+}. The OSL dose response function of the Tm-doped sample showed a linear response in the dose range of 1–10000 mGy.

1. Introduction

Storage phosphors have a function of storing the absorbed energy of ionizing radiation, such as X- or γ-rays, in the form of carrier trapping at localized trapping centers. When storage phosphors are irradiated by ionizing radiation, many electrons and holes corresponding to radiation energy are generated. These electrons and holes immediately recombine at a luminescence center to emit scintillation photons or are temporally stored at a trapping center.[1] Then, the stored electrons and holes are released upon stimulation with heat or light, resulting in photon emissions called thermally stimulated luminescence (TSL) or optically stimulated luminescence (OSL), respectively.[2] Using these properties, we can estimeate exposure dose because luminescence intensity depends on exposure dose.[3–5] Therefore, storage phosphors that exhibit TSL and OSL properties are used for radiation detectors in applications such as environmental dosimetry,[6] medical imaging,[7–9] and personal dosimetry.[10]

OSL-type storage phosphors have several advantages compared with TSL-type ones because OSL is observed by optical stimulation. Thus, the dose assessment time using OSL is generally shorter than that using TSL, which contributes to the lower cost of the reader system. In addition, OSL shows smaller thermal quenching than TSL because the readout of OSL is generally conducted at room temperature. C-doped Al_2O_3[11–13] and BeO[14] are well-known OSL-type storage phosphors with high sensitivity. However, despite these advantages, only

*Corresponding author: e-mail: takebuchi.yuma.ty1@ms.naist.jp
https://doi.org/10.18494/SAM.2020.2717

ISSN 0914-4935
https://myukk.org/

a few materials are used as OSL-type storage phosphors in practical applications. Therefore, new materials with a good dose sensitivity and response to radiation over a wide dose range are required. For this purpose, recently, we have introduced new OSL materials, such as Ce-doped CsCl,[3] Ce-doped $30Zn_3(PO_4)_2$-$70Al(PO_3)_3$,[15] Mn-doped $LiCa(Ga,Al)F_6$,[16] and rare-earth-doped $LiSrAlF_6$.[17]

To improve the intensity of the OSL signal, some fluoroperovskite-type materials that have ABF_3 compositions were investigated,[18–20] and Ce-doped $KMgF_3$ showed high sensitivity, even forty times than that of C-doped Al_2O_3.[21] However, it is necessary to use other elements other than K because K contains a radioactive isotope (^{40}K), which causes intrinsic radioactivity within crystals. For this reason, we focused on $NaMgF_3$. $NaMgF_3$ is fluoroperovskite crystal that does not include such radioactive isotope element, and can be used as a host material for doping some activators. Additionally, the effective atomic number (Z_{eff}) of $NaMgF_3$ (Z_{eff} = 10.4) is closer to that of human tissue (Z_{eff} = 7.29)[22] than to that of $KMgF_3$ (Z_{eff} = 14.9). As an activator, we focused on Tm since Tm is a candidate dopant for generating luminescence centers, and dosimetric properties were reported in some Tm-doped materials.[23,24]

In this study, we synthesized undoped and Tm-doped $NaMgF_3$ single crystals and investigated their OSL properties. In addition to OSL properties, scintillation properties were also investigated to identify the origin of luminescence.

2. Materials and Methods

Undoped and Tm-doped $NaMgF_3$ samples were synthesized by a simple solidification method. NaF (99%, Wako Pure Chemical Industries, Ltd.), MgF_2 (99.9%, Stella Chemifa Corporation), and TmF_3 (>99.99%, Stella Chemifa Corporation) were mixed homogeneously and put into a graphite crucible. The nominal concentration of Tm was 0.1% with respect to Mg. The crucibles were set in a stainless chamber and enclosed by a carbon resist heater. Most parts of the hot zone were made of high-purity carbon. After setting the crucibles at the hot zone, the chamber was evacuated up to 9.9×10^{-4} Pa, and CF_4 gas was injected to remove oxygen sources such as H_2O. Then, the crucible was heated to no less than the melting point (1030 °C) of $NaMgF_3$ and kept at this temperature for 3 h. The temperature in this equipment was roughly estimated from the supplied voltage, which was calibrated by melting other materials. After the sample synthesis, the wide surfaces of the obtained crystal were polished using a polishing machine (BUEHLER, MetaServ 250). To check the phase of the samples, their X-ray diffraction (XRD) patterns were measured in the range of 2θ = 10–80° with a diffractometer (Rigaku, MiniFlex600) using a CuKα X-ray microtube having a beryllium window supplied with a bias voltage of 40 kV and a tube current of 15 mA.

The X-ray-induced scintillation spectra were measured using our original set up.[25] The X-ray generator (Spellman, XRB80N100/CB) was equipped with an X-ray tube supplied with 40 kV and 1.2 mA. The X-ray tube has a tungsten anode target and a beryllium window. The irradiation dose for the samples was 540 mGy, which was calibrated using the ionizing chamber (PTW, TN30013). The scintillation light was led into the spectrometer (Andor, DU-420-BU2 CCD equipped with a Shamrock SR 163 monochromator) through a 2-m-long optical fiber (quarts

fiber, Mitsubishi Cable Industries, Ltd.) to obtain the spectrum. The CCD was cooled to 188 K by a Peltier module. The X-ray-induced scintillation decay time profiles were evaluated using the afterglow characterization system.[26] The wavelength sensitivity range of PMT was from 160–650 nm.

The OSL properties were investigated using the X-ray generator and spectrofluorometer (JASCO, FP8600). In our geometry, the irradiation dose was calibrated using an X-ray ionization chamber (TN30013, PTW). The stimulation and monitoring wavelengths were 470 and 360 nm, respectively. The stimulation wavelength was selected on the basis of other reports on the OSL properties of fluoroperovskite.[18,20] Before the measurement of the OSL spectrum, the sample was irradiated with X-rays of 1000 mGy. Then, the OSL dose response function was measured after X-ray irradiations at various doses from 0.1 to 10000 mGy.

3. Results and Discussion

Figure 1 shows a photograph of the undoped and Tm-doped $NaMgF_3$ samples after polishing their surfaces. The thickness of these samples was about 1 mm. Both samples were visibly transparent. The black region may have been generated by abrasives that entered into a crack. The Tm-doped sample was more opaque than the undoped sample, which may be due to the fine cracks formed during Tm doping. Figure 2 shows the XRD patterns of the two samples and the reference. Since the peak positions matched those of the reference, there were no impurity phases within the accuracy of the XRD measurement. The difference in peak ratio accounted for the setting errors of the samples because we evaluated bulk-form samples. By XRD analysis, we confirmed that the synthesized samples were a single-phase $NaMgF_3$, which belonged to the *Pbnm* space group of the orthorhombic crystal system.

Figure 3 shows the X-ray-induced scintillation spectra of both samples. The Tm-doped sample exhibited emission peaks at around 345, 360, 450, 480, 510, and 650 nm. These peaks were attributed to the $^1I_6$–$^3F_4$, $^1D_2$–$^3H_6$, $^1D_2$–$^3F_4$, $^1G_4$–$^3H_6$, $^1D_2$–$^3H_5$, and $^1D_2$–$^3H_4$ transitions of

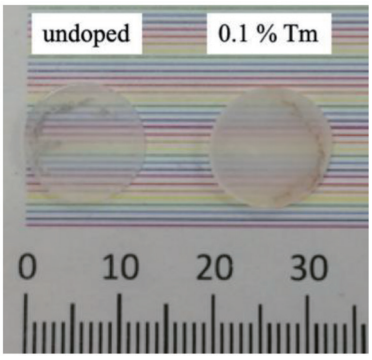

Fig. 1. (Color online) Photograph of undoped and Tm-doped samples.

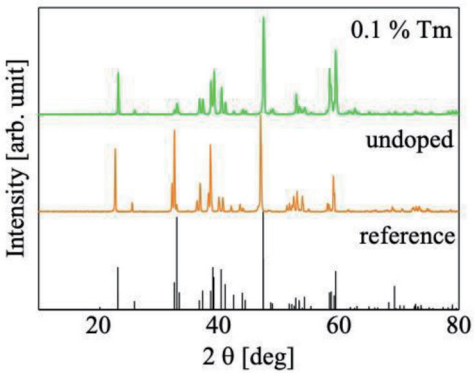

Fig. 2. (Color online) XRD patterns of undoped and Tm-doped $NaMgF_3$ samples and reference (COD.9001612).

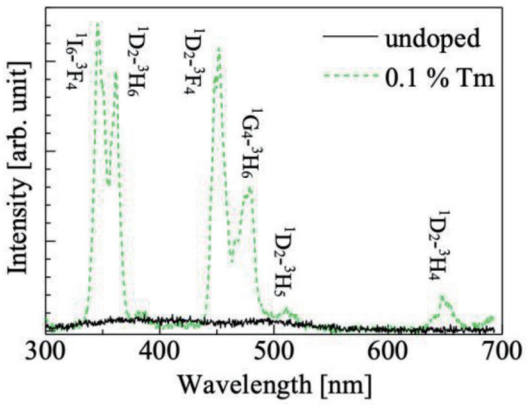

Fig. 3. X-ray-induced scintillation spectra of undoped and Tm-doped samples.

Tm^{3+}.[24,27] On the other hand, the undoped sample exhibited a broad emission peak from 300 to 550 nm. This emission peak is considered to be due to self-trapped excitons (STEs) and some types of defect.[28,29]

Figure 4 shows the X-ray-induced scintillation decay time profiles of the two samples. The decay time profiles of the undoped and Tm-doped samples were fitted by the sum of two exponential decay functions. The obtained decay time constants of the undoped and Tm-doped samples were 0.7 and 17 ns, and 0.15 and 1.1 ms, respectively. In the undoped sample, the primary decay time constant was attributed to an instrumental response, and the secondary decay time constant was attributed to STEs.[28] In the Tm-doped sample, the primary decay time constant was attributed to the 4f–4f ($^1G_4$–$^3H_6$) transitions of Tm^{3+}.[24] The secondary decay constant could not be attributed explicitly to any factor because the typical decay time constant of the 4f–4f transitions of Tm^{3+} was less than 300 μs.[27,30,31] However, some fluoride materials showed similar components in X-ray-induced scintillation decay time profiles.[24,32]

Figure 5 shows the OSL spectrum of the Tm-doped sample. The OSL peak was observed at around 360 nm upon 470 nm stimulation, and the peak position was consistent with the X-ray-induced scintillation spectrum of the Tm-doped sample. The emission origin is considered to be the $^1I_6$–$^3F_4$ and $^1D_2$–$^3H_6$ transitions of Tm^{3+}. The emission peak seemed to be a single line because of the low wavelength resolution of this measurement, although there are two emission origins. Figure 6 shows the OSL dose response function of the Tm-doped sample. The Tm-doped sample showed a linearity under X-ray irradiation between 1 and 10000 mGy with a typical error of ±10%. The linearity was not confirmed at 0.1 mGy since no emission peak was observed. As a result, the sensitivity of the 0.1% Tm-doped sample is lower than those of the Ce-doped $NaMgF_3$ and common dosimetric materials such as C-doped Al_2O_3 and BeO.[13,14,21] Thus, further improvement such as the investigation of different Tm concentrations is needed.

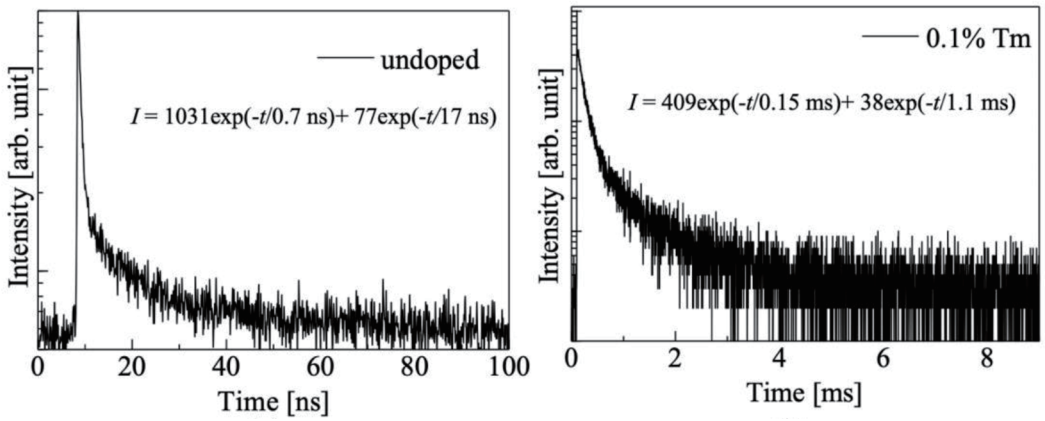

(a) (b)

Fig. 4. X-ray-induced scintillation decay time profiles of (a) undoped and (b) Tm-doped samples.

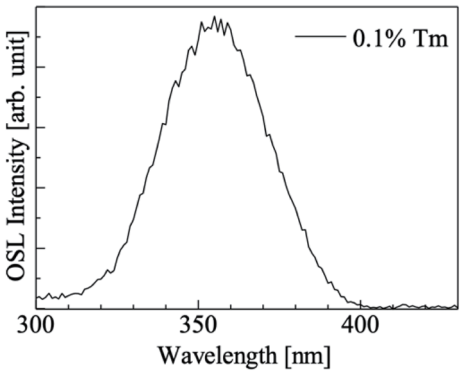

Fig. 5. OSL spectrum of Tm-doped sample upon 470 nm stimulation.

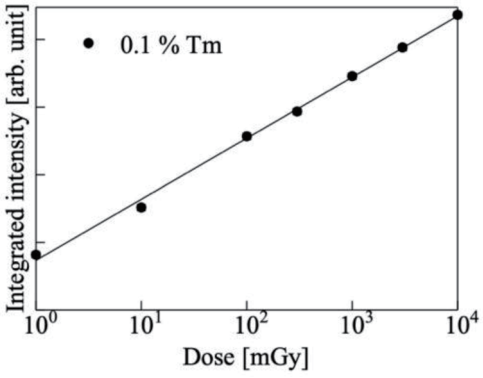

Fig. 6. OSL dose response function of Tm-doped sample.

4. Conclusions

We synthesized undoped and Tm-doped $NaMgF_3$ single crystals and investigated their scintillation and OSL properties. The XRD patterns of the synthesized samples were of the single phase. In the X-ray-induced scintillation spectra, the undoped sample showed emission bands of STE and some defects. By contrast, the Tm-doped sample showed some emission lines corresponding to the 4f–4f transitions of Tm^{3+}. In the X-ray-induced scintillation decay time profiles, the secondary decay time constant of the undoped sample is attributed to STEs, and the primary decay time constant of the Tm-doped sample is attributed to the 4f–4f transitions of Tm^{3+}. In the OSL spectrum, the Tm-doped sample showed emission considered to be due to the 4f–4f transitions of Tm^{3+}. The dose response function of the Tm-doped sample was confirmed and showed linearity under X-ray irradiation at doses of 1–10000 mGy.

Acknowledgments

This work was supported by Grants-in-Aid for Scientific Research A (17H01375) and B (18H03468 and 19H03533) and Young Scientists B (17K14911). The Cooperative Research Project of the Research Center for Biomedical Engineering, Iketani Foundation, Murata Foundation, and Nippon Sheet Glass Foundation are also acknowledged.

References

1 T. Yanagida: Proc. Japan Academy, Ser. B, Physical and Biological Sciences **94** (2018) 75.
2 T. Yanagida, G. Okada, and N. Kawaguchi: J. Lumin. **207** (2019) 14.
3 H. Kimura, F. Nakamura, T. Kato, D. Nakauchi, G. Okada, N. Kawaguchi, and T. Yanagida: Sens. Mater. **30** (2018) 1555.
4 N. Kawaguchi and T. Yanagida: Sens. Mater. **31** (2019) 1257.
5 T. Sakai, M. Koshimizu, Y. Fujimoto, D. Nakauchi, T. Yanagida, and K. Asai: Sens. Mater. **30** (2018) 1565.
6 K. Shin, M. Yuta, F. Akihiko, K. Haruki, A. Katsuya, K. Hironobu, T. Yoshinori, N. Hidehito, K. Toshio, K. Hitoshi, S. Masaaki, S. Yasuhiko, M. Kiyotaka, H. Kazuyuki, and Y. Takayoshi: Sens. Mater. **22** (2010) 377.
7 H. Nanto: Sens. Mater. **30** (2018) 327.
8 K. Shinsho, D. Maruyama, S. Yanagisawa, Y. Koba, M. Kakuta, K. Matsumoto, H. Ushiba, and T. Andoh: Sens. Mater. **30** (2018) 1591.
9 Y. Koba, R. Shimomura, W. Chang, K. Shinsho, S. Yanagisawa, G. Wakabayashi, K. Matsumoto, H. Ushiba, and T. Ando: Sens. Mater. **30** (2018) 1599.
10 R. W. Christy, N. M. Johnson, and R. R. Wilbarg: J. Appl. Phys. **38** (1967) 2099.
11 S. W. S. McKeever, M. Akselrod, and B. G. Markey: Radiat. Prot. Dosimetry **65** (1996) 267.
12 S. W. S. McKeever: Radiat. Meas. **46** (2011) 1336.
13 M. S. Akselrod, V. S. Kortov, D. J. Kravetsky, and V. I. Gotlib: Radiat. Prot. Dosimetry **33** (1990) 119.
14 M. Sommer, A. Jahn, and J. Henniger: Radiat. Meas. **43** (2008) 353.
15 S. Hirano, T. Kuro, H. Tatsumi, G. Okada, N. Kawaguchi, and T. Yanagida: J. Mater. Sci. Mater. Electron. **28** (2017) 6064.
16 T. Yanagida, K. Fukuda, G. Okada, K. Watanabe, and N. Kawaguchi: J. Mater. Sci. Mater. Electron. **28** (2017) 6982.
17 T. Yanagida, G. Okada, K. Fukuda, K. Watanabe, and N. Kawaguchi: Radiat. Meas. **106** (2017) 124.
18 D. J. Daniel, A. Raja, U. Madhusoodanan, O. Annalakshmi, and P. Ramasamy: Opt. Mater. **58** (2016) 497.
19 L. Camargo, L. P. Cruz, E. Cruz-Zaragoza, S. M. Ovalle, and J. Marcazzó: Appl. Radiat. Isot. **141** (2018) 219.
20 C. Dotzler, G. V. M. Williams, U. Rieser, and J. Robinson: J. Appl. Phys. **105** (2009) 1.
21 N. J. M. Le Masson, A. J. J. Box, C. W. E. Van Eijk, C. Furetta, and J. P. Chaminade: Radiat. Prot. Dosimetry **100** (2002) 229.
22 C. A. Jayachandran: Phys. Med. Biol. **16** (1971) 005.
23 N. Kawano, N. Kawaguchi, G. Okada, Y. Fujimoto, and T. Yanagida: Sens. Mater. **30** (2018) 1539.
24 N. Kawano, D. Nakauchi, K. Fukuda, G. Okada, N. Kawaguchi, and T. Yanagida: Jpn. J. Appl. Phys. **57** (2018) 102401.
25 T. Yanagida, K. Kamada, Y. Fujimoto, H. Yagi, and T. Yanagitani: Opt. Mater. **35** (2013) 2480.
26 T. Yanagida, Y. Fujimoto, T. Ito, U. Kor, and K. Mori: Appl. Phys. Express **7** (2014) 6.
27 L. Macalik, J. Hanuza, D. Jaque, and J. García Solé: Opt. Mater. **28** (2006) 980.
28 A. S. Voloshinovskii, V. B. Mikhailik, and P. A. Rodnyi: Radiat. Eff. Defects Solids **135** (1995) 281.
29 N. J. M. Le Masson, A. P. Vink, P. Dorenbos, A. J. J. Bos, C. W. E. VanEijk, and J. P. Chaminade: J. Lumin. **101** (2003) 175.
30 E. Cavalli, C. Meschini, A. Toncelli, M. Tonelli, and M. Bettinelli: J. Phys. Chem. Solids **58** (1997) 587.
31 J. Tang, Y. Chen, Y. Lin, and Y. Huang: J. Lumin. **138** (2013) 15.
32 F. Nakamura, T. Kato, G. Okada, N. Kawaguchi, K. Fukuda, and T. Yanagida: Ceram. Int. **43** (2017) 7211.